

NONLINEAR BUCKLING PREDICTIONS OF CURVED PANELS UNDER COMBINED COMPRESSION AND SHEAR LOADING

Moshe M. Domb

Bombardier Aerospace, Strategic Technology Group
Downsview, Ontario, Canada M3K 1Y5

Keywords: *curved panel, buckling, compression loading, shear loading*

Abstract

The present work deals with implementation of a nonlinear buckling analysis technique for the prediction of the initial buckling in simply-supported curved panels subjected to a combined loading state of compression and shear. Interaction buckling curves are generated for a wide range of curved panels. The curves include the effect of a pre-existing level of imperfection in the panel on the combined buckling characteristics.

Good correlation with the parabolic NACA interaction curve was obtained for the entire combined loading range when the model predictions are presented through the buckling stress ratios relative to the nonlinear pure-compression and pure-shear cases. The results presented in this work show the high sensitivity of curved panel buckling to the degree of initial imperfection in the panel, especially when compression loading is present. The magnitude of imperfection in a given panel would be dependent on the panel configuration parameters and its radius-to-thickness ratio. Detailed knowledge of this dependency would lead to better prediction of the buckling characteristics of the panel.

1. Introduction

The current sources of design information on the stability of shell structures are the Structures Monographs published by the National Aeronautics and Space Administration (NASA) in the 1960's [1-3]. These monographs provide design information in the form of empirical

knockdown factors and design recommendations for isotropic flat and curved panels. The factors represent lower bounds to experimental data available at that time, and they take into account the large scatter obtained in the test data. These corrections are done to account primarily for the high sensitivity of shell buckling to initial geometric imperfections in the structure. The NASA structural stability monographs and all the references from the 1940's and 1950's on which the monographs are based, provide a reliable but over-conservative means of designing shell structures. In addition, the applicability of the information to high-performance shell structures such as fibre-reinforced composites is limited. The design guidelines on shell stability given in the NASA monographs are widely used throughout the aerospace industry.

Many advances in the area of shell stability analysis have been accomplished since the days of the NASA monographs. At the same time, the availability today of modern and affordable computing resources has enabled the development of advanced computational structural analysis capabilities for the nonlinear analysis of shell structures. Therefore, it is evident that the information provided in the NASA monographs on shell stability, as it has also been indicated in Reference 4, need to be updated and expanded.

2. Current Approach and Objective

A nonlinear modelling technique for the buckling analysis of curved panels has been developed in-house. Implementation of this

technique for prediction of the initial buckling in simply-supported curved panels subjected to pure compression and pure shear has been reported recently in [5] and [6], respectively. In the above studies, nonlinear design curves were generated for each loading case, representing the corresponding buckling stress coefficient as a function of the non-dimensional curved panel parameter Z_b . The expression for Z_b is given by:

$$Z_b = (b^2/rt)(1-\nu^2)^{0.5} \quad (1)$$

where ν is the Poisson's ratio and b, r, t are the panel's width (circumferential dimension), radius and thickness. The present work deals with implementation of the above technique for the case of simply-supported curved panels subjected to combined compression and shear loading. The work consists of the generation of compression/shear interaction buckling curves for these panels. The software used here is the Finite Element code MSC.Marc, a commercial package known for its advanced nonlinear capabilities.

The currently used interaction curves for combined compression and shear buckling of simply-supported curved panels are presented in Figure 1 after the original source by NACA [7]. The interaction curve is represented by the parabola

$$R_s^2 + R_c = 1 \quad (2)$$

where R_s and R_c are given by:

$$R_s = F_s / (F_s)_0 \quad (3)$$

$$R_c = F_c / (F_c)_0 \quad (4)$$

In the above expressions, F_s, F_c are the shear and compression buckling stresses, respectively, for a particular loading ratio, and $(F_s)_0, (F_c)_0$ are the buckling stresses for the pure-shear and pure-compression cases, respectively. The above

figure also depicts numerous test data points gathered in the 1940's. Should be noted the large scatter in the test data in comparison to the parabolic relationship.

The objective of the present work is to generate refined interaction curves for combined compression/shear buckling of curved panels through the use of advanced nonlinear modelling techniques. The resulting curves will represent an update and expansion of the currently used interaction curves, and will address in particular the issue of initial geometric imperfections in the panel.

3. Model Description

A schematic view of a typical curved panel is depicted in Figure 2. Initial geometric imperfections in the panel are incorporated into the model through a coordinate perturbation in the radial direction for each node in the model. The imperfections are introduced in a way that their magnitude is described via a pre-defined imperfection coefficient a_0 . A detailed description of this imperfection methodology can be found in [5,6].

The loading strategy used to induce a combined state of compression and shear is presented in Figure 3. The figure depicts the definition of a combined loading parameter ϕ , which represents the angle in degrees in a combined axial/shear interaction plot along which the incremental loading is applied. In theory, the above parameter can assume values between 0° and 360° , however the results presented in the present study are limited to values of ϕ ranging from 0° for the pure compression case to 90° for the pure shear case. This range represents the first quadrant in an overall axial/shear interaction plot.

The combined loading is applied incrementally via prescribed axial and circumferential displacements on all edges of the panel. The incremental displacements for the case of flat panels are defined by:

$$\Delta v_0 = \alpha \Delta u_0 \quad (5)$$

$$\alpha = 2(1+\nu)\tan\phi[(F_s)_0 / (F_c)_0] \quad (6)$$

where $\Delta u_0, \Delta v_0$ are the incremental axial and transverse displacements at the main loading edge, respectively, $(F_s)_0, (F_c)_0$ are the theoretical buckling stresses for the pure-shear and pure-compression cases, respectively, ν is the material Poisson's ratio, and ϕ is the combined compression/shear loading parameter. For curved panels, the incremental displacements are:

$$\Delta\theta_0 = \alpha\Delta w_0 \quad (7)$$

$$\alpha = 2(1+\nu)\tan\phi(1/r)[(F_s)_0 / (F_c)_0] \quad (8)$$

In the above equations, $\Delta\theta_0$ is the incremental angle of rotation at the main loading edge to induce the shear loading, Δw_0 is the incremental axial displacement at the main loading edge, and r is the radius of the panel. All the kinematic loading edge conditions applied on the panel based on the above definitions are illustrated in Figure 4 for both flat and curved panels.

In the selection of the panels to be analyzed, a number of geometric and material parameters are pre-selected and kept constant for all panels. These parameters are the radius of curvature r , thickness t , aspect ratio a/b , Young's modulus E and Poisson's ratio ν . Specification of the curved panel parameter Z_b for the different panels subsequently determines the value of the corresponding panel width b (via Eq. 1) and panel length a .

3.1 Determination of the Buckling Load

The techniques typically used for the identification of the instant of buckling in curved panels are strongly dependent upon the global response of the panel during the loading procedure, which by itself depends on the specific configuration of the panel. For this purpose, three typical cases have been identified

in the current work, and they are depicted schematically in Figure 5.

The most straightforward and convenient approach would be to identify the instant of buckling directly from the panel's overall load-versus-displacement curve (or stress-versus-strain curve). One case of this kind of response, referred to as Case I, is characterized by an overall bilinear load-displacement dependency. The point of discontinuity in the slope represents the instant of buckling of the panel. A second case under the same approach, referred to as Case II, exhibits a very gradual reduction in stiffness (an almost linear curve) even at small load levels, followed by a sudden drop in the load. The peak load clearly represents the buckling load of the panel.

Unlike the first two cases, some panel configurations are characterized by a load-displacement curve which exhibits a nonlinear response immediately from the onset of loading, with a continuous reduction in the overall stiffness (Case III in Figure 5). In such a case, the critical buckling load cannot be pinpointed directly from an inspection of the load-deflection curve. Therefore, a different procedure must be applied. In this case, the development of the out-of-plane displacement as a function of the applied displacement loading is followed at the location in the panel which displays the largest deflection at the post-buckled stage. In mathematical terms, the instant of buckling for this case is identified when:

$$[\partial w_{cr} / \partial u_0] = \text{maximum} \quad (9)$$

where w_{cr}, u_0 are the out-of-plane deflection of the critical location in the panel and the applied displacement loading, respectively.

4. Model Results and Discussion

A variety of simply-supported panels with $r/t=1000$ and $a/b=4$ have been analyzed in the range $0 \leq Z_b \leq 100$ using the above methodology. As it was discussed in References [5,6], there is a strong dependency of the buckling stress on

the degree of initial imperfection in curved panels under any type of loading conditions, and in particular for panels in the intermediate ($7 < Z_b \leq 25$) and highly-curved ($25 < Z_b$) ranges. It is believed that the actual amount of imperfection in a given panel is dependent upon the curved panel parameter Z_b as well as on its r/t ratio [6]. For convenience purposes, a single normalized imperfection function was used in each curved panel configuration for every case of the combined loading parameter ϕ . This function was chosen to be the one corresponding to the loading case $\phi=45^\circ$. The magnitude of the imperfection in the panel is introduced via the imperfection parameter a_0 . A particular value of a_0 was selected for each of the panels analyzed in the present work based on the results presented in [5,6].

Thirteen panel configurations have been investigated. However, plots for only three representative cases are presented here. These correspond to the perfectly-flat case ($Z_b=0$) and curved panels with $Z_b=7$ and 15. Typical post-buckled shapes for these panels are depicted in Figures 6-8, respectively, corresponding to the combined loading case of $\phi=45^\circ$.

The predicted responses for the above panels are illustrated in Figures 9-11 through the compressive stress-versus-axial strain curves for eight values of ϕ ranging from 0° (pure compression) to 90° (pure shear). Similar curves (not shown here) could be generated also in terms of the shear stress-versus-shear strain.

The nonlinear results are also shown in Figures 12-14 in the form of R_s -versus- R_c interaction plots (defined in Equations 3 and 4), which is similar to the currently used interaction curve from NACA. The figures also show for reference the parabolic NACA curve based on Eq. 2, as well as a linear relationship curve. The nonlinear predictions for the shear and compression buckling stress ratios R_s, R_c are plotted in the above figures: (a) in relation to the theoretical (NACA, subscript "th") buckling stresses for the pure-shear and pure-compression cases:

$$(R_s)_{th} = F_s / (F_s)_{th} \quad (10)$$

$$(R_c)_{th} = F_c / (F_c)_{th} \quad (11)$$

and (b) in relation to the predicted nonlinear (subscript "fea") buckling stresses for the pure-shear and pure-compression cases:

$$(R_s)_{fea} = F_s / (F_s)_{fea} \quad (12)$$

$$(R_c)_{fea} = F_c / (F_c)_{fea} \quad (13)$$

The results reveal that for panels in the almost-flat range of $0 \leq Z_b \leq 7$ (which from practical manufacturing considerations are characterized by low levels of imperfection), the nonlinear predictions using values of $a_0 \leq 0.02$ correlate very well with the parabolic reference curve for the entire range $0^\circ \leq \phi \leq 90^\circ$ (see Figures 12 and 13). It should be noted that this is regardless of which of the above approaches is used to calculate the buckling stress ratios R_s and R_c .

For intermediate ($7 < Z_b \leq 25$) and highly-curved ($Z_b > 25$) panels (see representative case in Figure 14), the nonlinear predictions, when plotted using the buckling stress ratio pair $(R_s)_{th}$ and $(R_c)_{th}$, diverge significantly from a parabolic relationship in the compression-dominated loading region ($\phi < 45^\circ$). This large discrepancy might be a consequence of the high sensitivity of compression buckling on the choice of imperfection distribution function in the above range of curved panels. Conversely, in the segment where shear is dominant ($45^\circ \leq \phi \leq 90^\circ$), the model results, although higher than the NACA estimates, exhibit a dependency much closer to parabolic than the compression-dominated cases. In the above ranges of panels, When the model predictions are presented, however, using the buckling stress ratio pair $(R_s)_{fea}$ and $(R_c)_{fea}$, the interaction buckling curve is very close to parabolic for the entire combined loading range $0^\circ \leq \phi \leq 90^\circ$.

The previous studies conducted for the pure-compression and pure-shear loading cases [5,6] have indicated a certain degree of conservatism in the currently used NACA design curves for panels in the highly-curved range. This observation is also reflected in the results presented in this work, and primarily in the compression-dominated loading region. It is recommended that a parabolic relationship be used for the buckling interaction curve of curved panels under combined compression and shear loading, however through the use of the buckling stress ratios $(R_s)_{fea}$ and $(R_c)_{fea}$ calculated relative to the nonlinear predictions for the pure-compression and pure-shear cases.

5. Concluding Remarks

A nonlinear modelling technique for the prediction of the initial buckling in simply-supported curved panels under combined compression and shear loading has been presented. Interaction buckling curves were generated for curved panels in the range $0 \leq Z_b \leq 100$, and they include the effect of a pre-existing level of imperfection in the panel on the combined buckling characteristics.

The nonlinear interaction predictions, when presented through the buckling stress ratio pair $(R_s)_{fea}$ and $(R_c)_{fea}$, were found to correlate well with the parabolic NACA curve for the entire range $0^\circ \leq \phi \leq 90^\circ$.

It is important to remember that curved panel buckling is extremely sensitive to the degree of initial imperfection in the panel, especially when compression loading is present. In addition, the magnitude of imperfection in a given panel would be dependent upon the curved panel parameter Z_b as well as on its radius-to-thickness ratio. Detailed knowledge of this dependency would lead to better prediction of the buckling characteristics of the panel.

6. References

[1] Anonymous. *Buckling of thin-walled circular cylinders*. NASA Space Vehicle Design Criteria (Structures), NASA SP-8007, September 1965.

[2] Anonymous. *Buckling of thin-walled truncated cones*. NASA Space Vehicle Design Criteria (Structures), NASA SP-8019, September 1968.

[3] Anonymous. *Buckling of thin-walled doubly-curved shells*. NASA Space Vehicle Design Criteria (Structures), NASA SP-8032, August 1969.

[4] Nemeth M P, and Starnes Jr. J H. *The NASA Monographs on Shell Stability Design Recommendations - A Review and Suggested Improvements*. NASA TP-1998-206290, January 1998.

[5] Domb M M and Leigh B R. Refined design curves for compressive buckling of curved panels using nonlinear finite element analysis. *42nd AIAA/ASME/ASCE/AHS/ASC Structures, Structural Dynamics and Materials Conference*, Seattle, Washington, USA, Paper #2001-1348, April 2001.

[6] Domb M M and Leigh B R. Refined design curves for shear buckling of curved panels using nonlinear finite element analysis. *43rd AIAA/ASME/ASCE/AHS/ASC Structures, Structural Dynamics and Materials Conference*, Denver, Colorado, USA, Paper #2002-1257, April 2002.

[7] Schilderout M and Stein M. *Critical Combinations of Shear and Direct Axial Stress for Curved Rectangular Panels*. NACA TN-1928, August 1949.

[8] Batdorf S B, Schilderout M and Stein M. *Critical Combinations of Shear and Longitudinal Direct Stress for Long Plates with Transverse Curvature*. NACA TN-1347, June 1947.

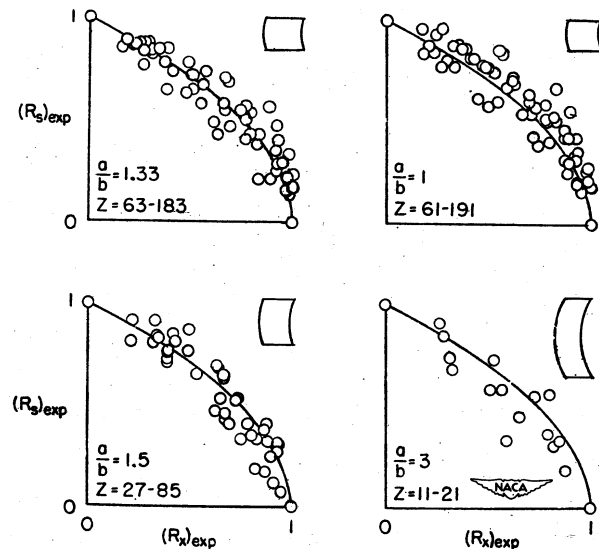


Figure 1 - Test results for buckling of curved rectangular panels under combined compression and shear loading and comparison to the parabola $R_s^2 + R_c^2 = 1$ [7].

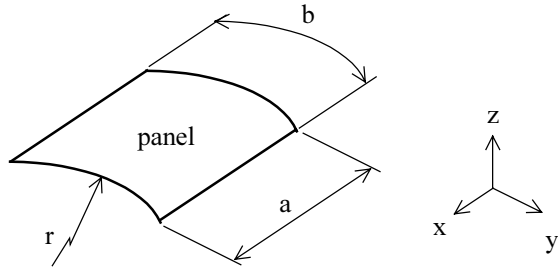


Figure 2 – Typical curved panel configuration.

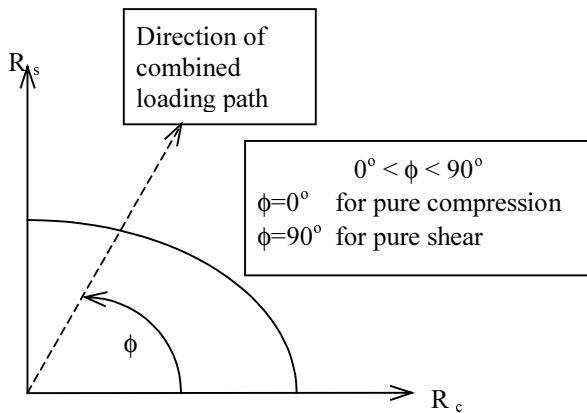


Figure 3 – Schematic of the combined compression and shear loading strategy.

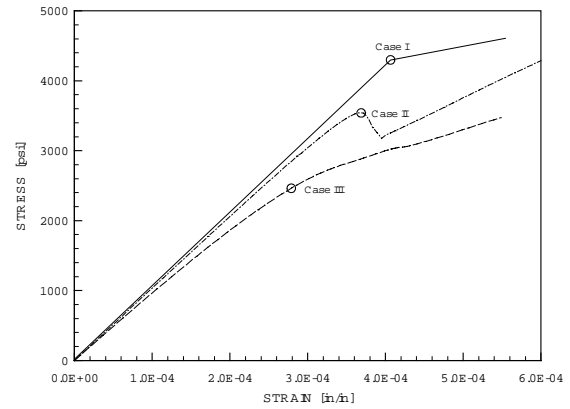


Figure 5 - The Various Cases Encountered in the Prediction of the Stress-versus-Strain Curve for a Simply-Supported Curved Panel, and the Identification of the Corresponding Buckling Stress.

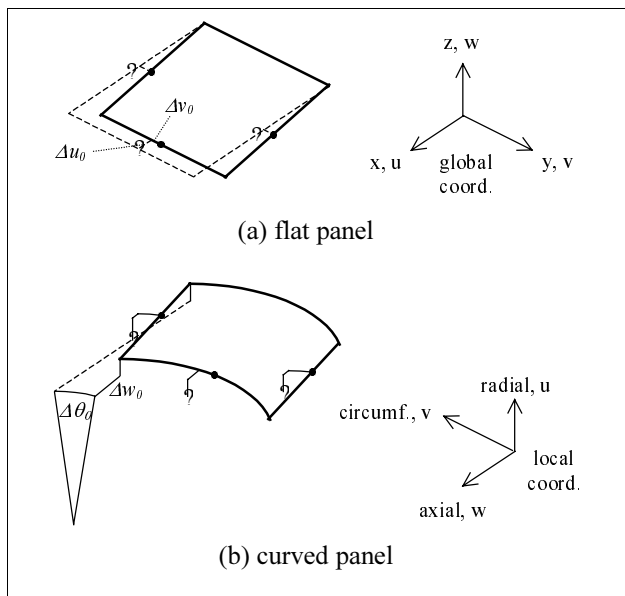


Figure 4 – Definition of the kinematic loading edge conditions used for the introduction of combined compression and shear loading in (a) flat and (b) curved panels.

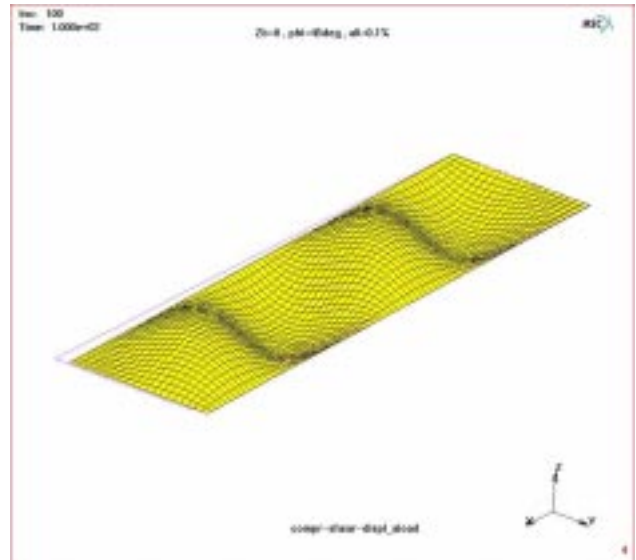


Figure 6 – Deformed shape at the post-buckled stage of a simply-supported flat panel ($Z_b=0$) with $r/t=1000$ and imperfection parameter $a_0=0.001$ under combined compression and shear loading ($\phi=45^\circ$).

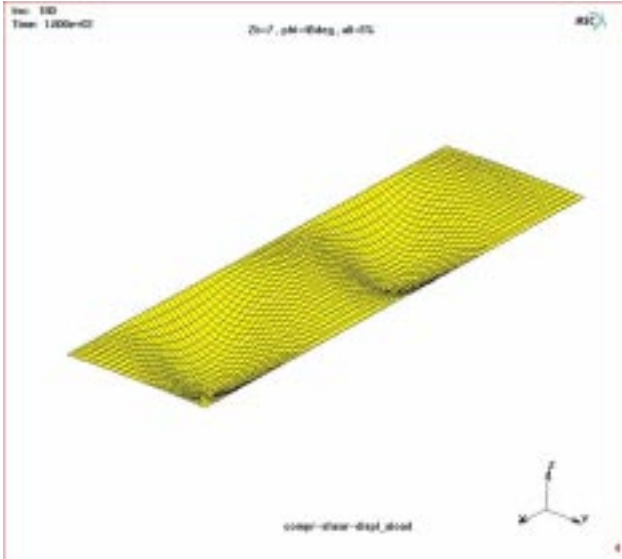


Figure 7 - Deformed shape at the post-buckled stage of a simply-supported curved panel ($Z_b=7$) with $r/t=1000$ and imperfection parameter $a_0=0.05$ under combined compression and shear loading ($\phi=45^\circ$).

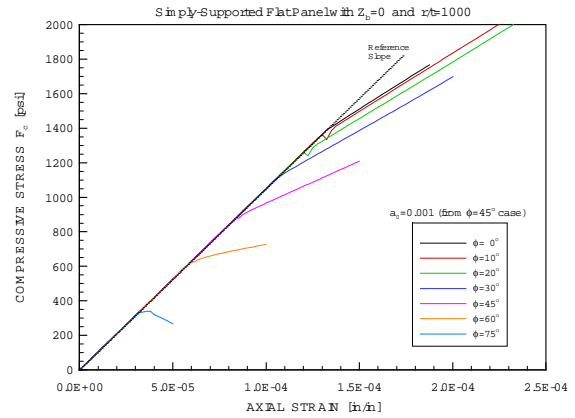


Figure 9 - Predicted compressive stress-strain curve for a simply-supported flat panel ($Z_b=0$) with $r/t=1000$ and imperfection parameter $a_0=0.001$ as a function of the shear/compression combined loading angle ϕ .

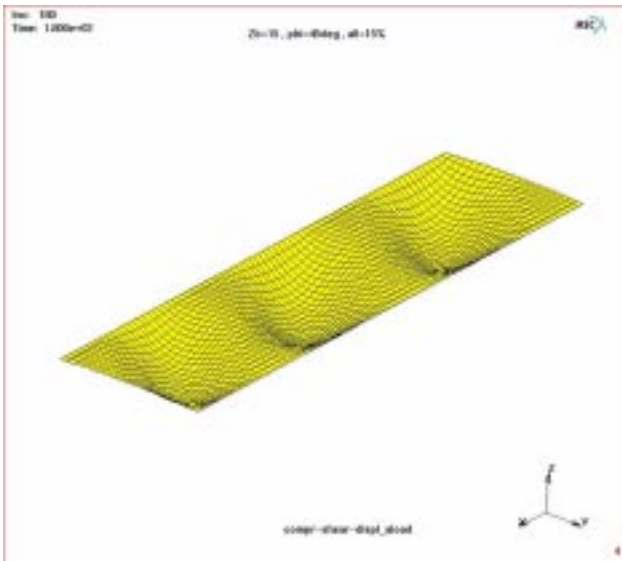


Figure 8 - Deformed shape at the post-buckled stage of a simply-supported curved panel ($Z_b=15$) with $r/t=1000$ and imperfection parameter $a_0=0.15$ under combined compression and shear loading ($\phi=45^\circ$).

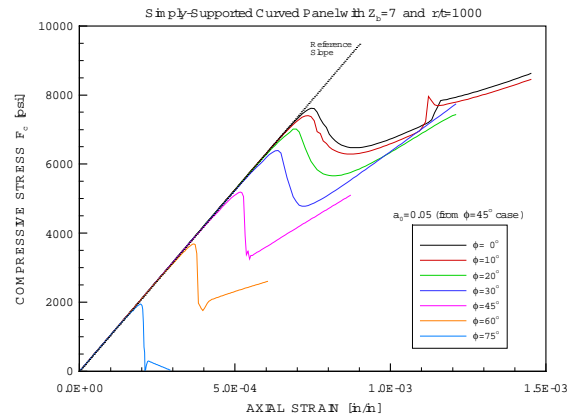


Figure 10 - Predicted compressive stress-strain curve for a simply-supported curved panel with $Z_b=7$, $r/t=1000$ and imperfection parameter $a_0=0.05$ as a function of the shear/compression combined loading angle ϕ .

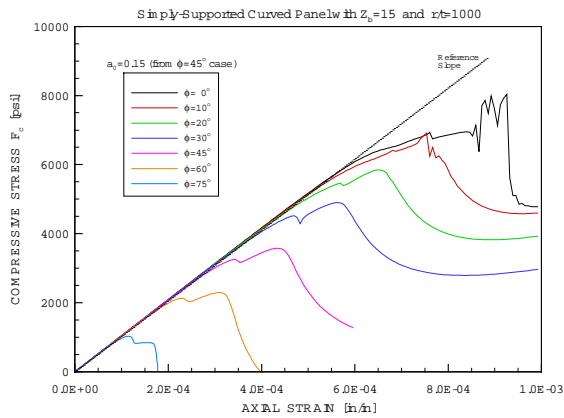


Figure 11 – Predicted compressive stress-strain curve for a simply-supported curved panel with $Z_b=15$, $r/t=1000$ and imperfection parameter $a_0=0.15$ as a function of the shear/compression combined loading angle ϕ .

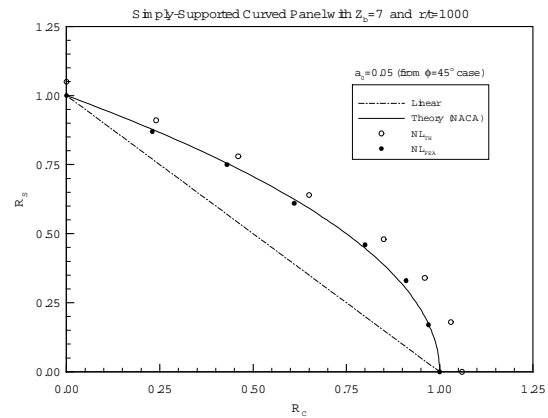


Figure 13 - Predicted shear/compression interaction buckling for a simply-supported curved panel with $Z_b=7$, $r/t=1000$ and imperfection parameter $a_0=0.05$ in the combined loading angle range $0^\circ \leq \phi \leq 90^\circ$.

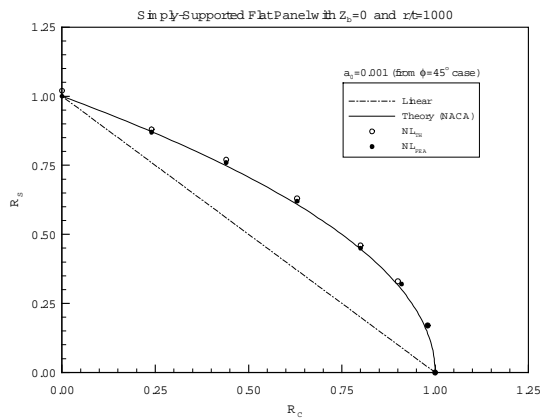


Figure 12 - Predicted shear/compression interaction buckling for a simply-supported flat panel ($Z_b=0$) with $r/t=1000$ and imperfection parameter $a_0=0.001$ in the combined loading angle range $0^\circ \leq \phi \leq 90^\circ$.

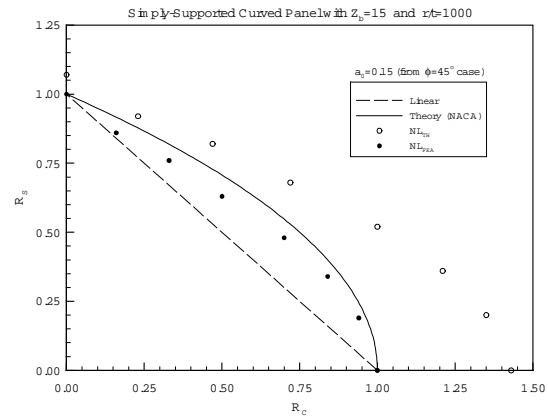


Figure 14 - Predicted shear/compression interaction buckling for a simply-supported curved panel with $Z_b=15$, $r/t=1000$ and imperfection parameter $a_0=0.15$ in the combined loading angle range $0^\circ \leq \phi \leq 90^\circ$.